Electronic Supplementary Material (ESI) for Journal of Materials Chemistry C.

Supporting Information

The Role of the Degree of Polymerization in the Chiroptical Properties of Dynamic Asymmetric Poly(diphenylacetylene)s

Juan José Tarrío,[a] Berta Fernández,[b] Emilio Quiñoá[a] and Félix Freire[a,*]

[a.] Centro Singular de Investigación en Química Biolóxica e Materials Moleculares (CiQUS) and Departamento de Química Orgánica. Universidade de Santiago de Compostela. Santiago de Compostela 15782, Spain.

[b.] Departamento de Química Física. Universidade de Santiago de Compostela. Santiago de Compostela 15782, Spain.

*Correspondence to felix.freire@usc.es

Table of Contents

Materials and Methods

CD measurements were done in a Jasco-720. The amounts of polymer used for CD measurements were 0.5 mg/mL in DMF and $CHCl_3$.

IR studies were carried out in a FTIR Varian 670 equipped with an ATR (GladiATR model) with diamond crystal of PIKE Technologies.

Raman spectra were performed in a Renishaw confocal Raman spectrometer (Invia Reflex model), equipped with two lasers (diode laser 785 nm and Ar laser 514 nm).

GPC studies were carried out in a Waters Alliance equipped with Phenomenex GPC columns. The amount of polymer used for GPC measurements was 0.5 mg/mL.

For molecular modeling we used Spartan 14 (MMFF94). As a molecular visualization system, we used PyMOL. The additional methodology used in the computational study is detailed in the Computational Details section.

Synthesis of Monomer and Polymers

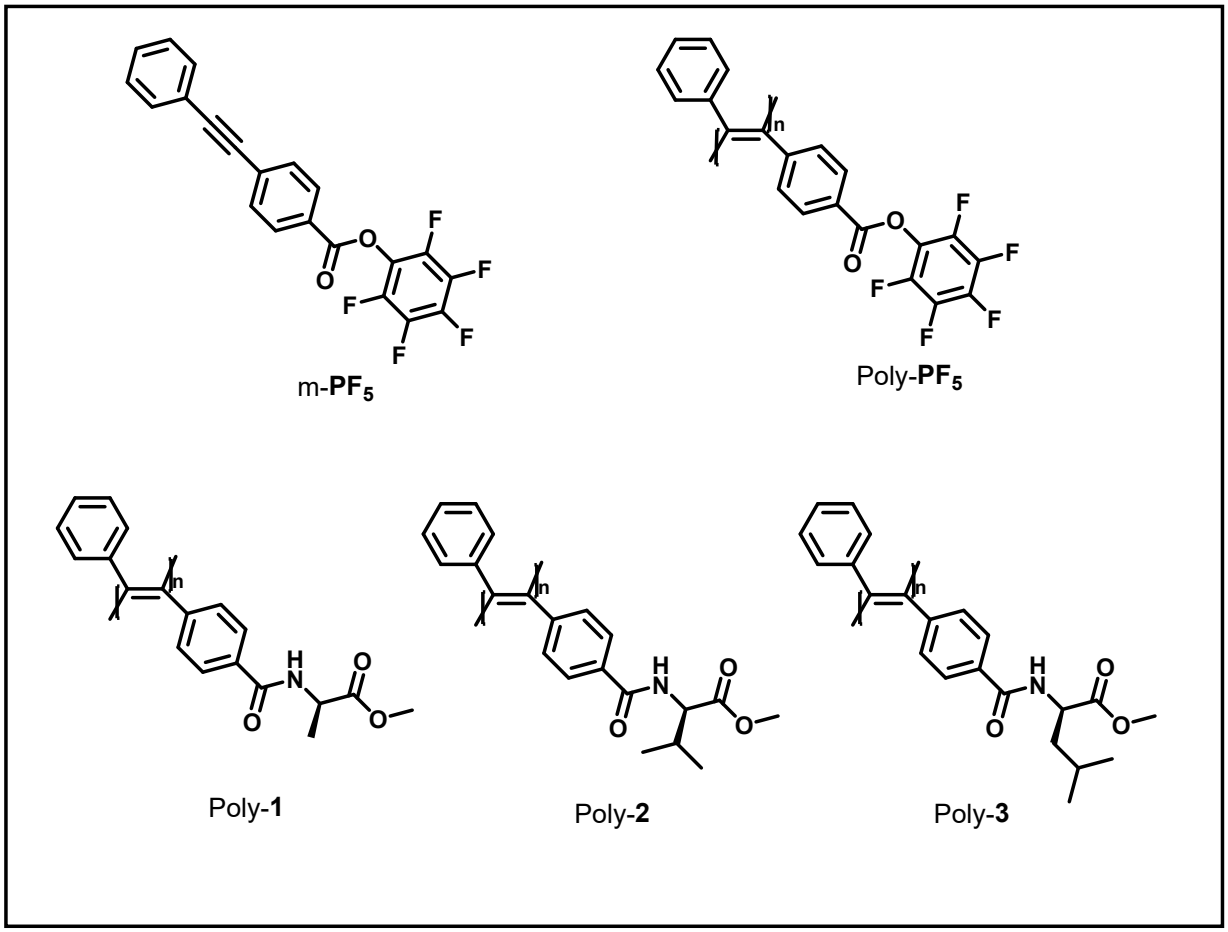

Figure S1: Structure of compounds m-**PF$_5$**, Poly-**PF$_5$** poly-**1**, poly-**2**, poly-**3**.

For preparation of m-**PF$_5$** and its polymerization, as well as the post-polymerization couplings procedure, see SI of Ref. **S1**.

NMR, Raman and IR studies of the polymers

The comparative NMR, IR and Raman spectra of short and large polymers showing the same structure pattern are shown below.

In Raman studies, the C=C bond stretching in the *trans* polymers shows an intensive peak at 1550 cm^{-1} and a decrease in the band at 1570-1585 cm^{-1} assigned to *cis* polymers.

IR experiments show a > 1 ratio between I_{1500}/I_{1450} that is ascribed to a *trans* configuration of different poly(acetylene)s and poly(phenylacetylene)s [Ref. **S2**].

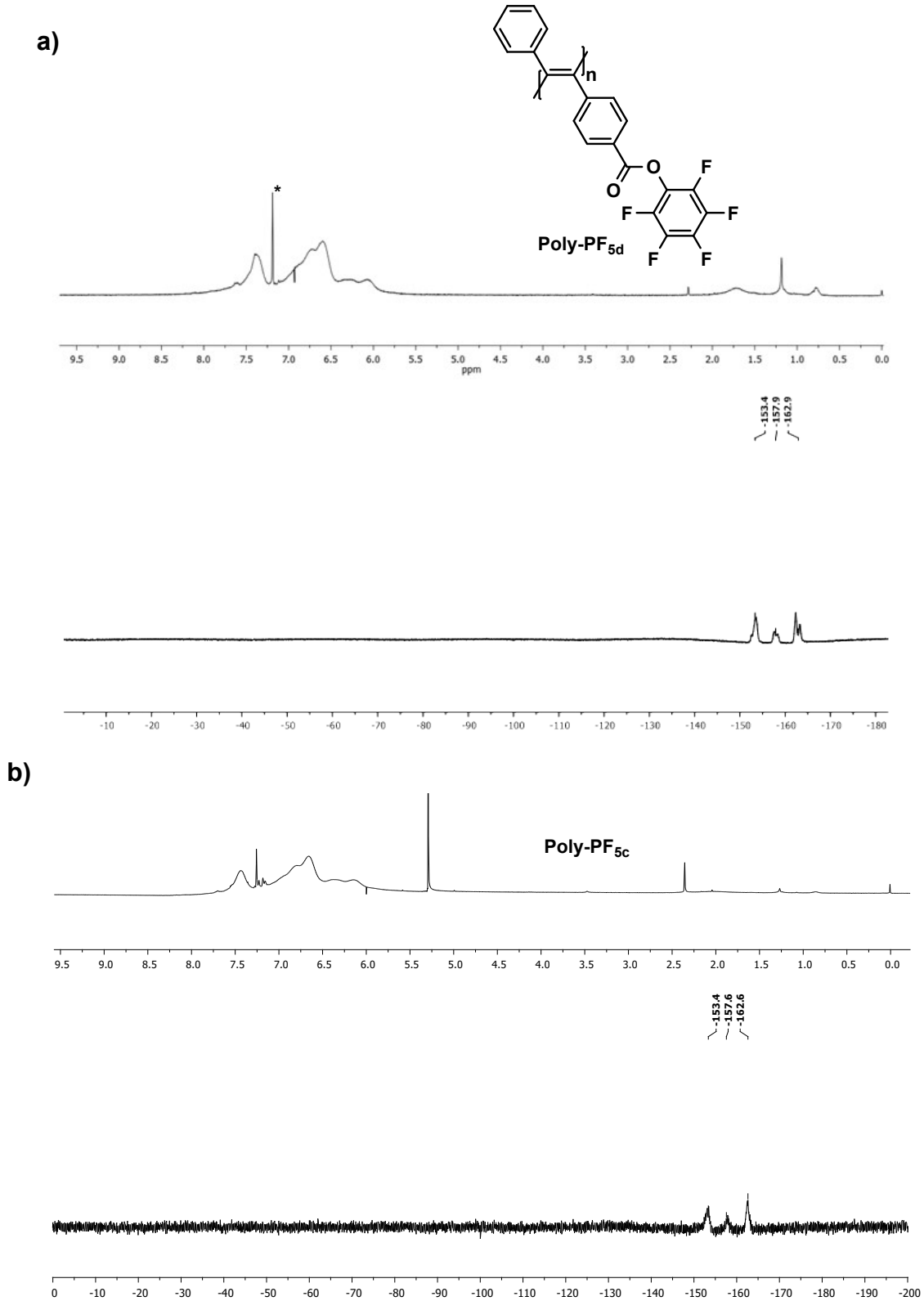

Figure S2. ^{1}H-NMR and ^{19}F-NMR spectra in $CDCl_3$ of a) Poly-**PF_{5d}** and b) Poly-**PF_{5c}**.

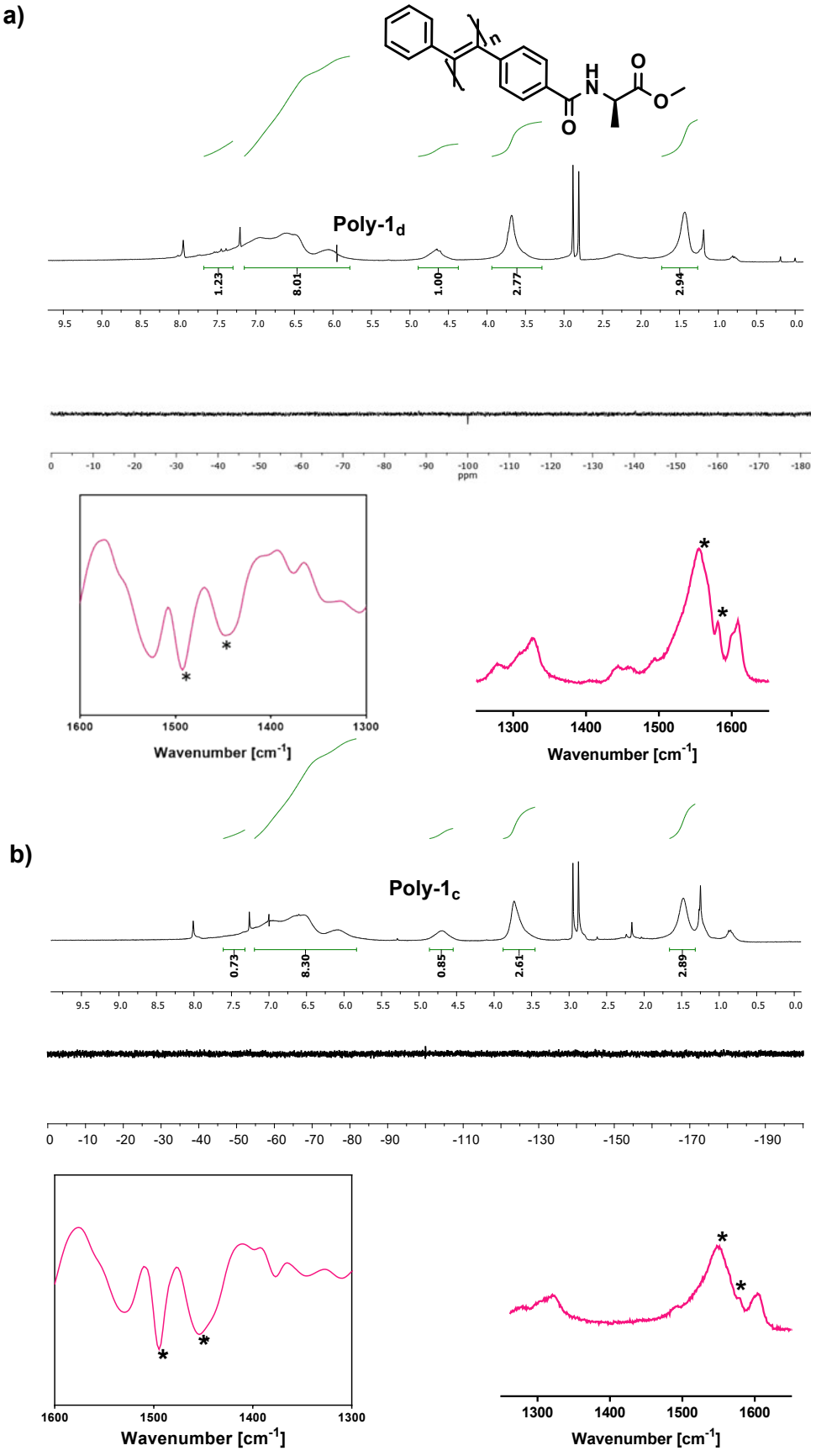

Figure S3. ^{1}H-NMR and ^{19}F-NMR spectra in $CDCl_3$, IR and Raman spectra of a) Poly-**1**$_d$ and b) Poly-**1**$_c$.

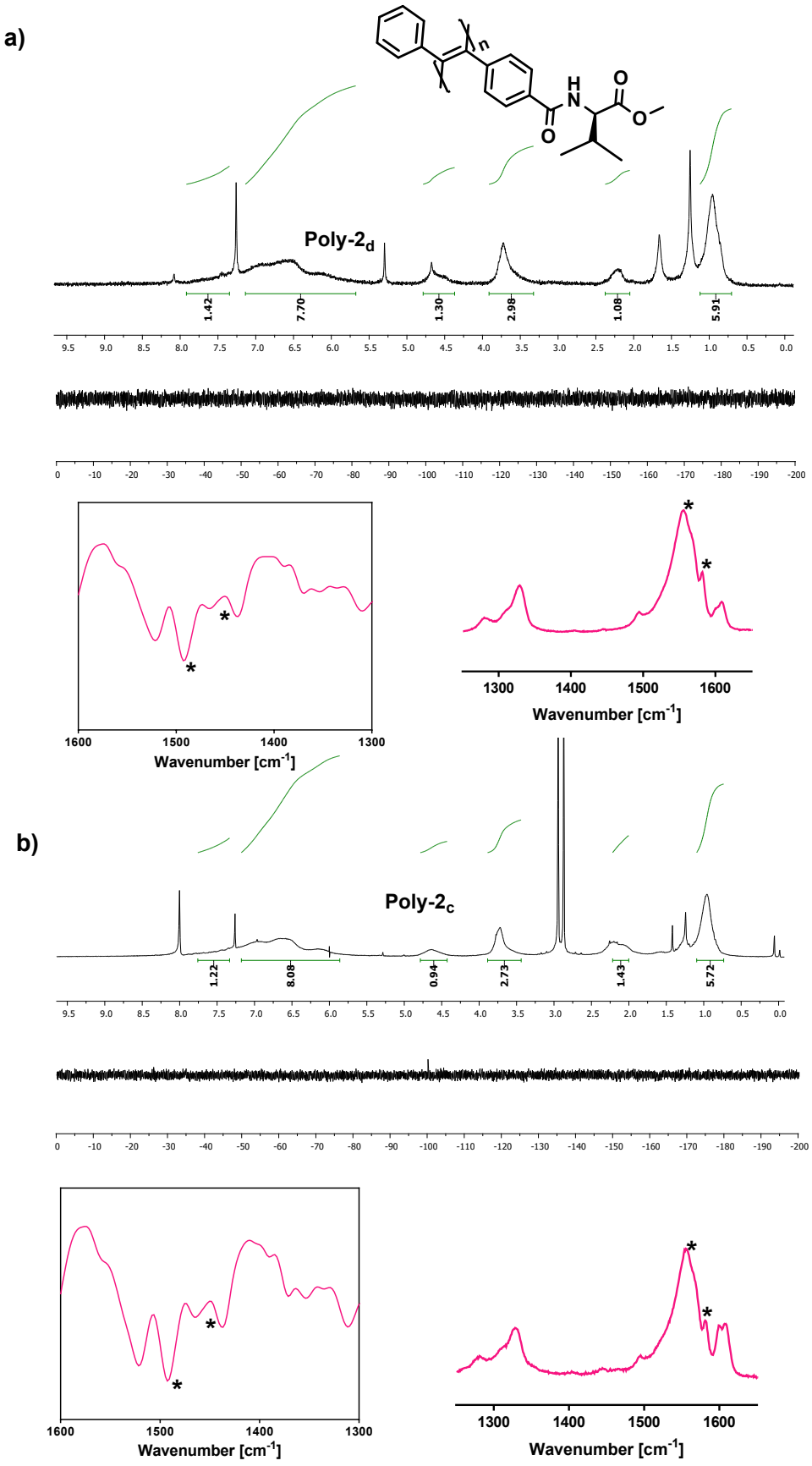

Figure S4. ^{1}H-NMR and ^{19}F-NMR spectra in $CDCl_3$, IR and Raman spectra of a) Poly-**2**$_d$ and b) Poly-**2**$_c$.

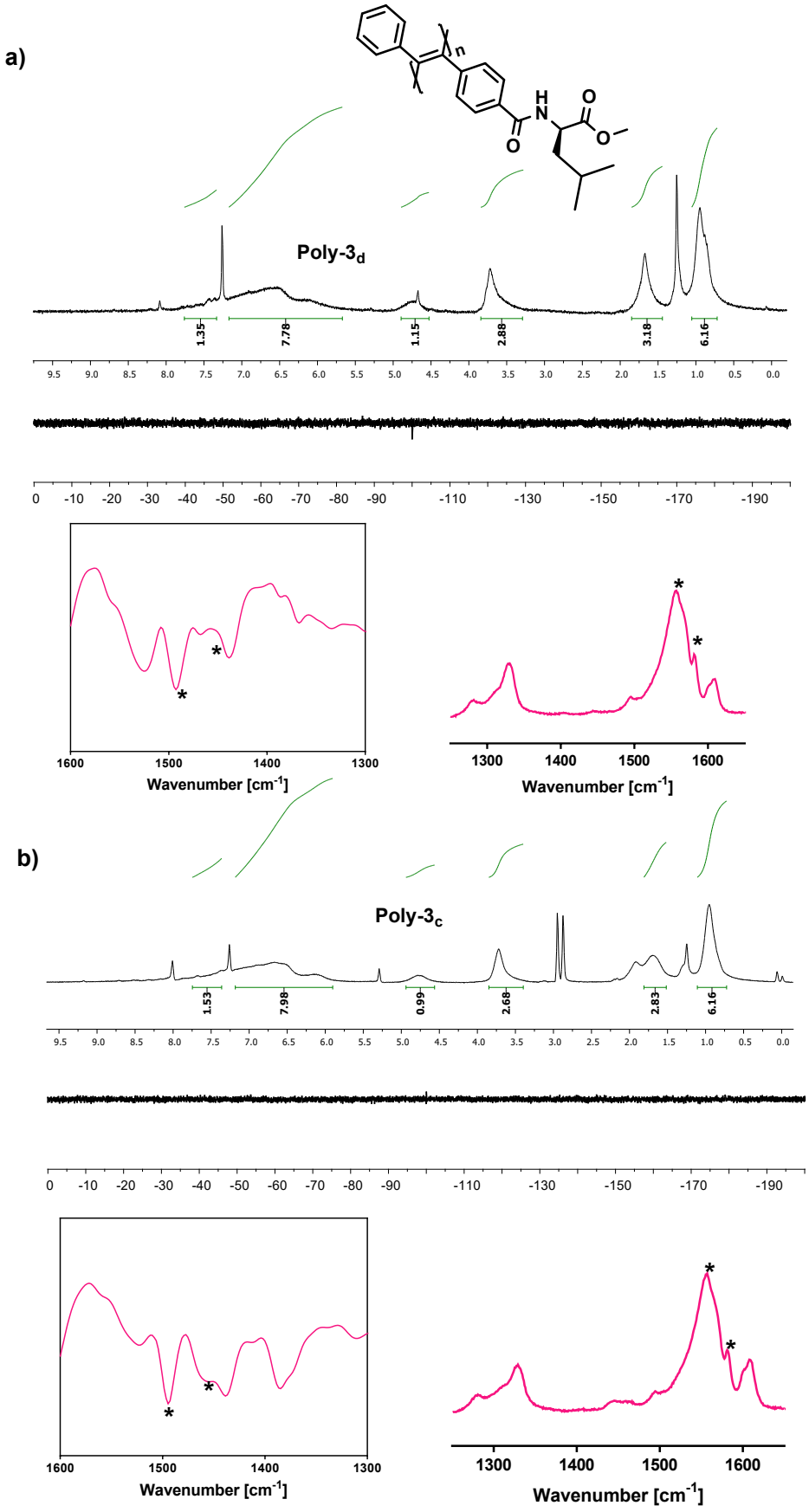

Figure S5. ^{1}H-NMR and ^{19}F-NMR spectra in $CDCl_3$, IR and Raman spectra of a) Poly-**3$_d$** and b) Poly-**3$_c$**.

CD Measurements

CD spectra in DMF (Figure 2 main text) and $CHCl_3$ are opposite for poly-(**1-3**) at different lengths. This is due to the different conformational composition adopted by the pendant group in polar (syn conformer, DMF) and low polar (anti conformer, $CHCl_3$). As a result, the spatial orientation of the amino acid side chain varies, producing a helix inversion in the PDPA. See reference 29 for details.

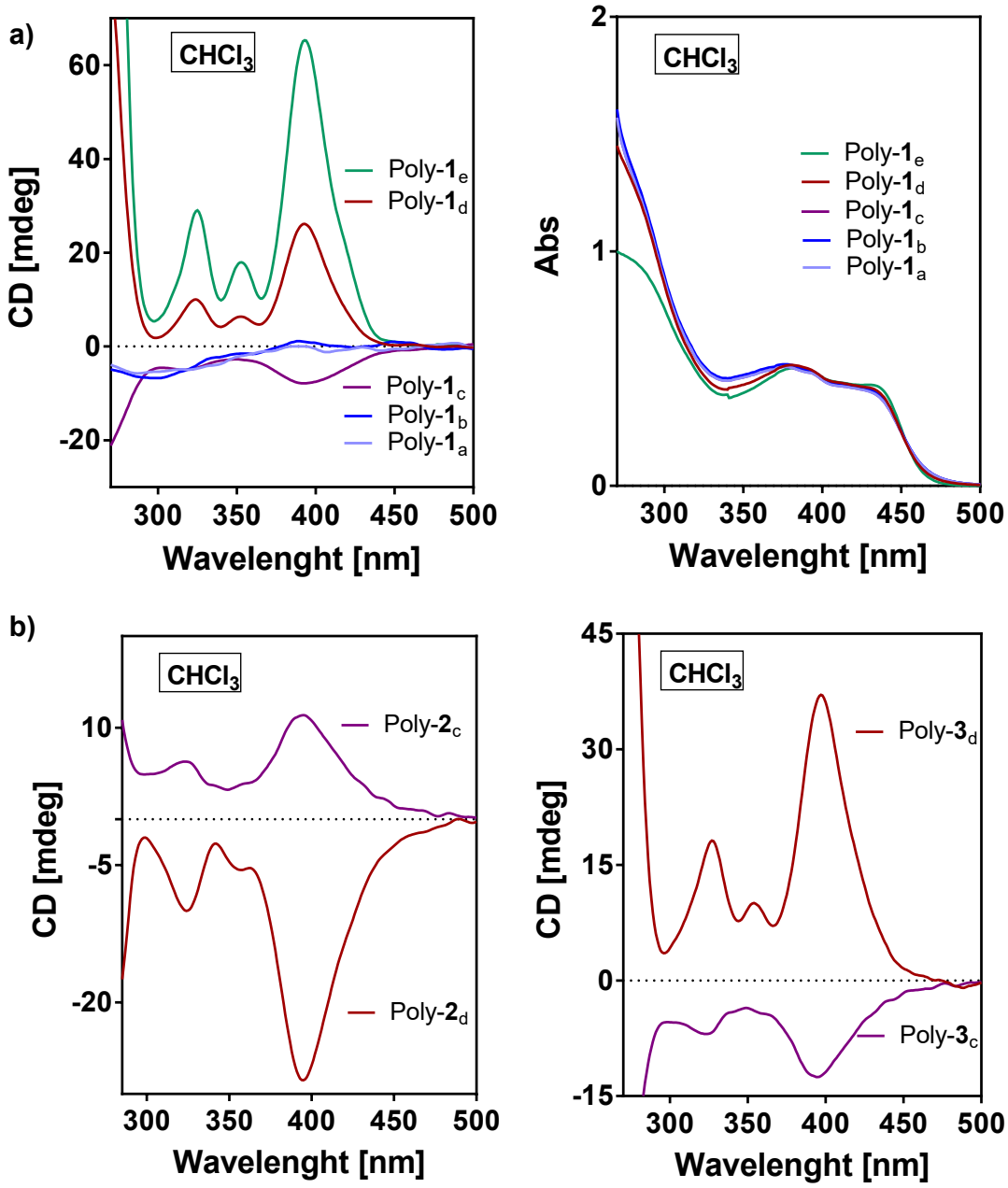

Figure S6: a) CD and UV measurements of 0,5 mg/mL solutions of poly-$\mathbf{1}_{a\text{-}e}$ in $CHCl_3$ after thermal annealing at 80 ºC during 24 h. b) CD measurements of 0,5 mg/mL solutions of poly-$\mathbf{2}_{c,d}$ and poly-$\mathbf{3}_{c,d}$ in $CHCl_3$ after thermal annealing at 80 ºC during 24 h.

Computational Details

Considering the difficulties to carry out theoretical calculations on large polymers, we resorted to the use of a reduced-size representative oligomer with 8 to 16 monomer repeating units.

The input structures used for the ECD calculations were adjusted according to the results obtained from structural techniques such as Raman, IR and AFM [Ref **S1a**]. Different 12-mer structures changing ω_1 and ω_3 dihedral angles and with ω_2 = 180º were calculated (see Figure 1b in the manuscript for dihedral angle definitions). From these results we selected the 12-mer defined by ω_1 = 165º and ω_3 = 110º due to its lower energy (Table S1) and the better agreement with the experimental CD.

Table S1. DFT(CAM-B3LYP)/3-21G electronic energies of the 12-mers. Angles are given in degrees

12-mer (ω_1-ω_3)	Energy (a.u.)
165-110	-6434.0798114
165-140	-6432.7030308
170-110	-6433.7370503
170-135	-6432.2250039

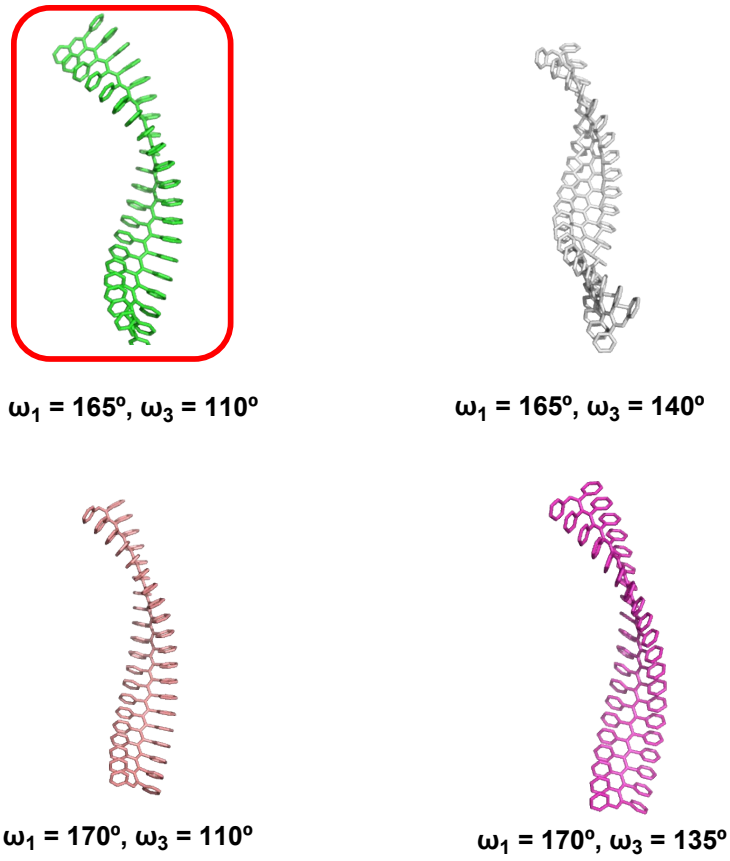

Figure S7: Different 20-mer structures calculated varying the ω_1 and ω_3 dihedral angles.

Methodology Applied

The choice of the methodology used to carry out the ECD calculations was determined by the size of the polymers under investigation. Considering this, time-dependent density functional theory (TD-DFT, Ref. **S3**) was the most efficient choice available, and we used it together with the CAM-B3LYP density functional (Ref. **S4**) and the 3-21G basis set (Ref. **S5**). We included 80 excitation energies in the calculations. This combination of density functional and basis set was selected based on density functional and basis set selection studies carried out in previous work, where it provided ECD and UV spectra for polyphenylacetylenes (PPAs) in an efficient way in terms of computational cost and reproducibility of the experimental spectra (Refs. **S6** and **S7**). The use of larger bases results prohibitive in the case of the considered polymers. Moreover, gas phase theoretical optimizations of the initial structures provided oligomers with a pitch that did not agree with the experimental AFM results.

The energies and ECD spectra were evaluated with the ORCA program (Ref. **S8**). To plot the spectra we used the GABEDIT program (Ref. **S9**) and for the density differences Avogadro (Ref. **S10**). For the ECD spectra we included 80 excitation energies in the calculations and employed lorentzian curves for the spectra. An isovalue of 0.003 was used to get the transition density differences. No solvent effects were included in the calculations.

Correlation between the Electronic Transfer and the Sign of the Transition Band

A tendency in the origin of the electron transfer and the sign of the corresponding transition band in the spectra can be observed. Thus, for a short oligomer with n = 8, electron transfer starts on the polyenic skeleton, whereas when the oligomer is larger (n = 12) electron transfer takes places mainly from the phenyl rings. In the intermediate cases, for instance when n = 10, a different behavior is observed. Here, both contributions are almost equally important showing an alternated spectrum that resembles those of PPAs.

We report in Figure S8 the main transitions involved in the different spectral bands for the spectra of the n = 8, 10 and 12 oligomers. In going from the 10- to the 12-mer the change in sign in the positive bands at around 350 and 450 nm can be attributed to excitations with larger negative intensity in the 12-mer spectrum, like those to the 44^{th} and the 58^{th} states.

To analyse these results further, we evaluated the electron density differences for the corresponding main excitations. The calculated electron density differences indicate that electron transfer from the phenyl substituents to the main skeleton takes place upon excitation in the 10-mer and the 12-mer, but the opposite trend occurs in the case of the 8-mer.

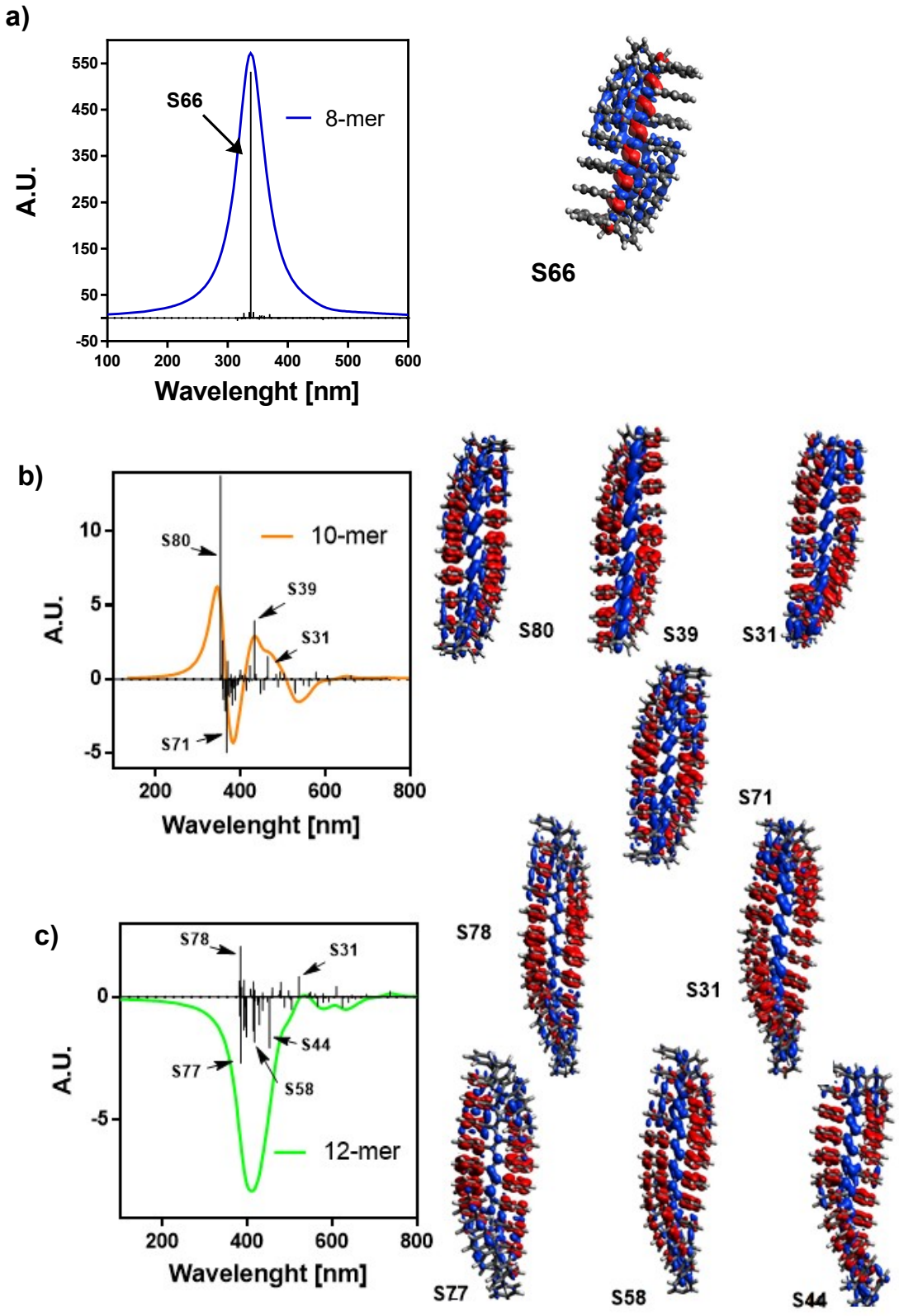

Figure S8: TD-DFT (CAM-B3LYP)/3-21G ECD spectra and electron density differences for the a) 8-mer b) 10-mer and c) 12-mer oligomers with ω1 (ω3)= 165 (110) degrees, showing the excited states (xth in Sx) that participate in the principal transitions within the main bands. Half width at half height equals 28 nm. No correction factors are included in the spectra. (red color negative and blue positive, isovalue equals 0.0003).

Influence of the ω_4 variation

Table S2. DFT(CAM-B3LYP)/3-21G electronic energies of 16-mers ω_1= 165º, ω_2= 180º and w3= 110º. Angles are given in degrees.

16-mer (ω_4)	Energy (a.u.)
-160	-11261.3811695
-120	-11260.4477777
0	-11261.3534380
40	-11261.1576255

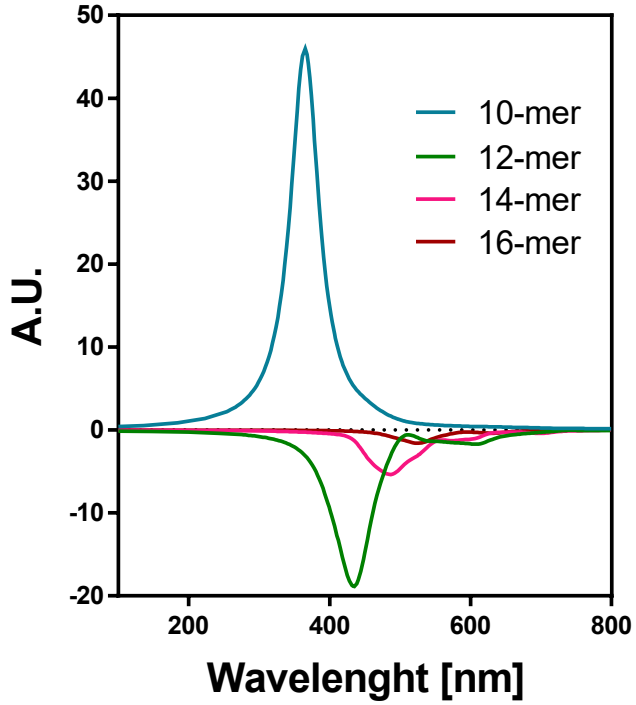

Figure S9: TD-DFT (CAM-B3LYP)/3-21G ECD spectra for the 10-,12-,14- and 16-mer with ω_1 (ω_3) ω_4 = 165 (110) -160 degrees. Half width at half height equals 25 nm. Intensities have been divided by a factor of 10 for the 10-mer.

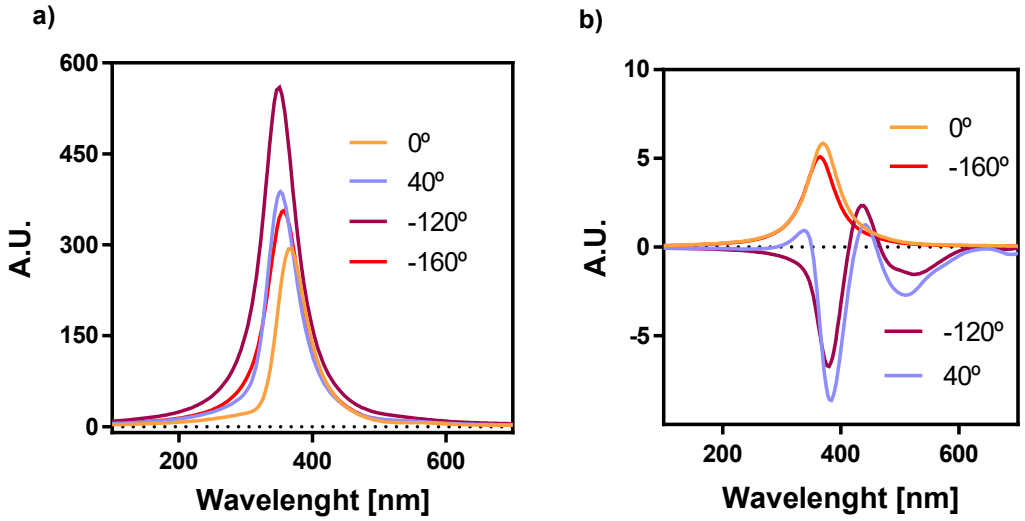

Figure S10: TD-DFT (CAM-B3LYP)/3-21G ECD spectra for the a) 8-mer and b) 10-mer with ω_1 (ω_3) = 165 (110) degrees changing ω_4. Half width at half height equals 25 nm.

PA and PPA calculations

We evaluated the corresponding ECDs for n= 8, 10, 12, 14, 16, 18, 20 and 100 for trans PA and for n= 8, 10, 12, 14, 16, 18, 20 and 25 for trans PPA.

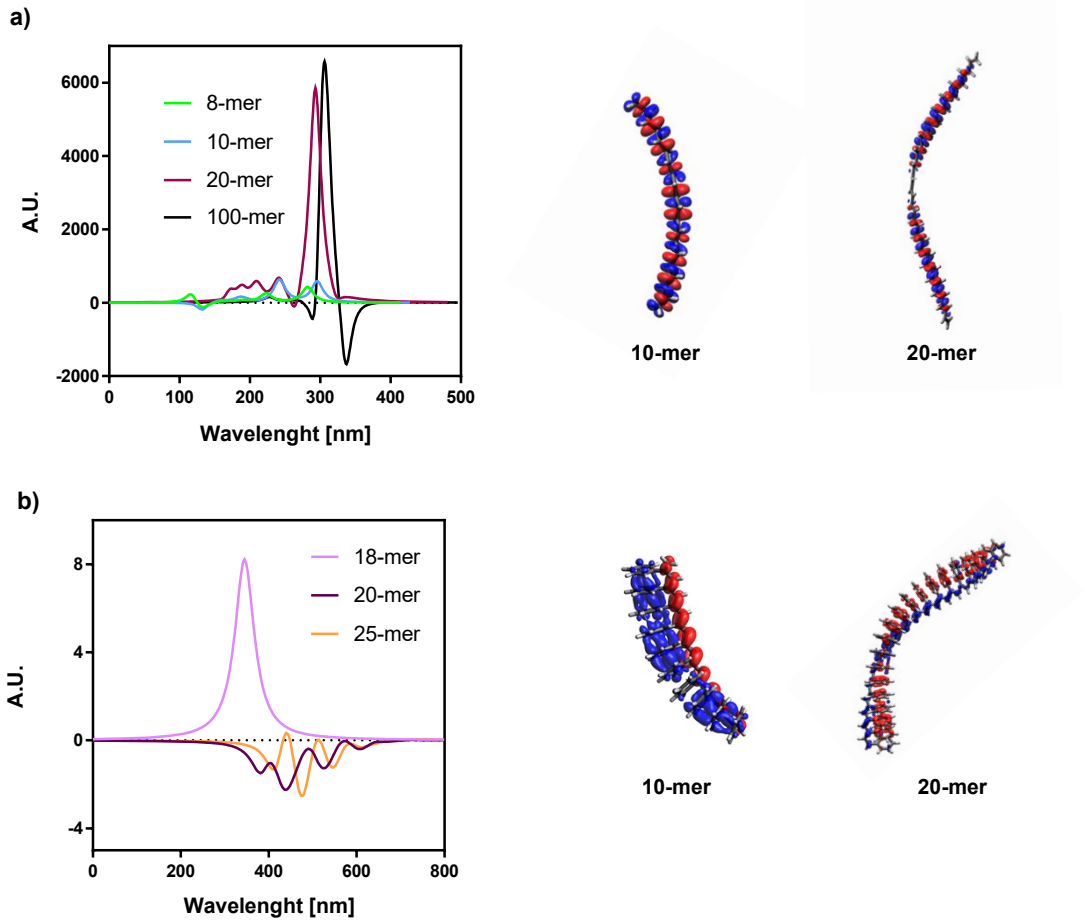

Figure S11. TD-DFT (CAM-B3LYP)/3-21G ECD spectra for the a) 8-,10-, 20- and 100-mer *trans* PA with ω_1 = 165 degrees and b) for the 18-, 20- and 25-mer *trans* PPA with ω_1 (ω_3)= 165 (110) degrees. Half width at half height equals 10 nm for *trans* PA and 27 nm for *trans* PPA. Intensities have been divided by a factor of 100 for the 18-mer PPA and by a factor of 10 for 100-mer PA.

Supporting References

S1. a) Tarrío, J. J.; Rodríguez, R.; Fernández, B.; Quiñoá, E.; Freire, F. Dissymmetric Chiral Poly (diphenylacetylene) s: Secondary Structure Elucidation and Dynamic Luminescence. *Angew. Chem. Int. Ed.*, **2022**, *61*, e202115070. b) Zhang, X. A.; Qin, A.; Tong, L.; Zhao, H.; Zhao, Q.; Sun, J. Z., Tang, B. Z. Synthesis of functional disubstituted polyacetylenes bearing highly polar functionalities via activated ester strategy. *ACS Macro Letters*, **2012**, *1*, 75-79.

S2. Simionescu, C. I.; Percec, V. Progress in Polyacetylene Chemistry. *Prog. Polym. Sci.*, **1982**, *8*, 133-214.

S3. Runge, E.; Gross, E. K. U. Density-Functional Theory for Time-Dependent Systems. *Phys. Rev. Lett.* **1984**, *52*, 997-1000.

S4. Yanai, T.; Tew, D. P.; Handy, N. C. A new hybrid exchange–correlation functional using the Coulomb-attenuating method (CAM-B3LYP). *Chem. Phys. Lett.*, **2004**, *393*, 51-57**.**

S5. Binkley, J. S.; Pople, J. A.; Hehre, W. J. Self-consistent molecular orbital methods. 21. Small split-valence basis sets for first-row elements. *J. Am. Chem. Soc.*, **1980**,*102*, 939-947.

S6. Fernández, B.; Rodríguez, R.; Rizzo, A.; Quiñoá, E.; Riguera, R.; Freire, F. Predicting the Helical sense of Poly(phenylacetylene)s from their Electron Circular Dichroism Spectra. *Angew. Chem. Int. Ed.* **2018**, *57*, 3666-3670.

S7. Fernández, Z.; Fernández, B.; Quiñoá, E.; Freire, F. The Competitive Aggregation Pathway of an Asymmetric Chiral Oligo (p-phenyleneethynylene) Towards the Formation of Individual P and M Supramolecular Helical Polymers. *Angew. Chem. Int. Ed.*, **2021**, *60*, 9919-9924.

S8. Neese, F. The ORCA program system. *WIREs Comput Mol Sci*. **2012**, *2*, 73-78.

S9. Gaussian 16, Revision C.01, Frisch, M. J.; Trucks, G. W.; Schlegel, H. B.; Scuseria, G. E.; Robb, M. A.; Cheeseman, J. R.; Scalmani, G.; Barone, V.; Petersson, G. A.; Nakatsuji, H.; Li, X.; Caricato, M.; Marenich, A. V.; Bloino, J.; Janesko, B. G.; Gomperts, R.; Mennucci, B.; Hratchian, H. P.; Ortiz, J. V.; Izmaylov, A. F.; Sonnenberg, J. L.; Williams-Young, D.; Ding, F.; Lipparini, F.; Egidi, F.; Goings, J.; Peng, B.; Petrone, A.; Henderson, T.; Ranasinghe, D.; Zakrzewski, V. G.; Gao, J.; Rega, N.; Zheng, G.; Liang, W.; Hada, M.; Ehara, M.; Toyota, K.; Fukuda, R.; Hasegawa, J.; Ishida, M.; Nakajima, T.; Honda, Y.; Kitao, O.; Nakai, H.; Vreven, T.; Throssell, K.; Montgomery, J. A., Jr.; Peralta, J. E.; Ogliaro, F.; Bearpark, M. J.; Heyd, J. J.; Brothers, E. N.; Kudin, K. N.; Staroverov, V. N.; Keith, T. A.; Kobayashi, R.; Normand, J.; Raghavachari, K.; Rendell, A. P.; Burant, J. C.; Iyengar, S. S.; Tomasi, J.; Cossi, M.; Millam, J. M.; Klene, M.; Adamo, C.; Cammi, R.; Ochterski, J. W.; Martin, R. L.; Morokuma, K.; Farkas, O.; Foresman, J. B.; Fox, D. J. Gaussian, Inc., Wallingford CT, **2016**.

S10. Allouche, A. R. Gabedit—A graphical user interface for computational chemistry softwares. *J. Comput. Chem.* **2011**, *32*, 174-182.

S11. Hanwell, M. D.; Curtis, D. E.; Lonie, D. C.; Vandermeersch, T.; Zurek, E.; Hutchison, G. R. Avogadro: an advanced semantic chemical editor, visualization, and analysis platform. *Journal of Cheminformatics* **2012**, *4*, 17.